QT interval Adaptation to Heart Rate Changes in Atrial Fibrillation as a Predictor of Sudden Cardiac Death

Alba Martín-Yebra, Leif Sörnmo, *Fellow, IEEE*, Pablo Laguna, *Fellow, IEEE*

Abstract— Objective: **The clinical significance of QT interval adaptation to heart rate changes has been poorly investigated in atrial fibrillation (AF), since QT delineation in the presence of f-waves is challenging. Therefore, the objective of the present study is to investigate new techniques for QT adaptation estimation in permanent AF. *Methods:* A multilead strategy based on generalized periodic component analysis is proposed for QT delineation, involving a spatial, linear transformation which emphasizes T-wave periodicity and attenuates f-waves. QT adaptation is modeled by a linear, time-invariant filter, whose impulse response describes the dependence between the current QT interval and the preceding RR intervals, followed by a memoryless, possibly nonlinear, function. The QT adaptation time lag is determined from the estimated impulse response. *Results:* Using simulated ECGs in permanent AF, the transformed lead was found to offer more accurate QT delineation and time lag estimation than did the original ECG leads for a wide range of f-wave amplitudes (the time lag estimation error was found to be -0.2±0.6 s for SNR = 12 dB). In a population with chronic heart failure and permanent AF, the time lag estimated from the transformed lead was found to have the strongest, statistically significant association with sudden cardiac death (SCD) (hazard ratio = 3.49), whereas none of the original, orthogonal leads had any such association. *Conclusions:* Periodic component analysis provides more accurate QT delineation and improves time lag estimation in AF. A prolonged adaptation time of the QT interval to heart rate changes is associated with a high risk for SCD. *Significance:* This study demonstrates that SCD risk markers, originally developed for sinus rhythm, can also be used in AF, provided that T-wave periodicity is emphasized. The time lag is a potentially useful marker for identifying patients at high risk for SCD, guiding clinicians in adopting effective therapeutic decisions.**

A. Martín-Yebra and P. Laguna are with the Biomedical Signal Interpretation & Computational Simulation (BSICoS) group, Aragón Institute of Engineering Research (I3A), Zaragoza University, Zaragoza, Spain, and Centro de Investigación Biomédica en Red de Bioingeniería, Biomateriales y Nanomedicina (CIBER-BBN), Spain, (e-mail: amartiny@unizar.es).
L. Sörnmo is with the Department of Biomedical Engineering, Lund University, Lund, Sweden.

Index Terms— **QT interval adaptation, ventricular repolarization, atrial fibrillation, sudden cardiac death.**

I. INTRODUCTION

THE clinical significance of impaired adaptation of the QT interval to changes in heart rate (HR) has been demonstrated in patients with myocardial infarction and ischemia as well as in those with long QT syndrome [1]– [6]. It is well-known that the adaptation is faster during HR acceleration than during deceleration ("hysteresis") and composed of two phases: a fast, initial phase extending a few RR intervals and a slow phase extending several minutes. The larger the change in HR the more pronounced is the hysteresis phenomenon and the longer extend the two phases [7]. In healthy subjects, it has been shown that the intrasubject variability of the QT-RR relation is low, whereas the intersubject variability is substantial, thus motivating subject-specific analysis [8].

The problem of how to quantify QT adaptation has been addressed by assuming that the dependence of the current QT interval on the preceding RR intervals can be modeled by a linear, time-invariant filter followed by a nonlinear, memoryless function [9]– [14]. This particular model structure was introduced in a much earlier study for the purpose of analyzing the QT-RR relation during exercise testing [15]. However, and most importantly, in that study the model parameters accounted only for the fast phase and were held fixed for all subjects, whereas, in [9]– [14], the model parameters were estimated from the observed RR intervals in each subject. The linear, time-invariant filter was defined by either a finite impulse response [9] or an infinite impulse response of a first-order system [12], [13]. From a large set of physiologically plausible nonlinear functions, the function providing the best fit to the QT-RR data was selected. The well-known Bazett's and Fridericia's formulas for QT interval correction were found inadequate as nonlinear functions [16], especially at low and high HRs. Various tailored approaches have been proposed for parameter estimation, based on, e.g., an unscented Kalman filter [10] or a cost function designed to minimize the fluctuations of the corrected QT intervals [12].

Parameter estimation is preferably performed in situations when the HR changes abruptly, e.g., during exercise testing, pacing at different rates, or changes in orthostatic position, as such situations help trigger both the fast and the slow phases. In unprovoked situations, several hours of ambulatory ECG

recordings may be needed to ensure a reasonably broad range of RR intervals so that accurate parameter estimates can be produced. For an increasingly broader range of RR intervals, the QT-RR relation becomes increasingly nonlinear [12].

A few studies have investigated QT adaptation in AF, involving either semi-automated or automated QT measurements obtained from 24-h Holter recordings. Some of these studies adopted the analysis pioneered in [15], i.e., using a filter with fixed coefficients to model cardiac memory [17], [18], while others confined the analysis to using Bazett's formula on the immediately preceding RR interval [19]. It should be emphasized that none of these AF-focused studies employed subject-specific analysis.

Due to the presence of f-waves in certain ECG leads, especially V1 and V2, delineation of the QT interval in AF recordings may be a challenging problem [20]. Most clinical studies have bypassed this challenge by simply analyzing a lead with negligible f-wave presence. When more than one lead is available, a multilead strategy based on periodic component analysis (πCA) [21], [22] may be used, taking advantage of the spatial redundancy among the different leads and the quasi-periodic structure of the ECG signal. This technique searches for the lead transformation maximizing the desired periodicity, while attenuating components with other periodicities, including f-waves. While this technique has been successfully applied to T-wave alternans detection [23] and quantification of T-wave morphological markers in sinus rhythm [24], it remains to be demonstrated whether the analysis of QT adaptation in AF patients benefits from πCA.

A novelty of the present study is the exploration of a generalized variant of πCA to achieve robust estimation of the adaptation time lag. Other novelties relates to the evaluation of performance: a simulation model to generate ECG signals in AF is used to evaluate the errors associated with QT delineation and time lag estimation, and a population with chronic heart failure (CHF) and permanent AF [25] is used to assess the prognostic value of the time lag used for predicting sudden cardiac death (SCD).

The paper is organized as follows. Section II describes the multilead strategy used to robustify QT delineation and QT adaptation. Section III describes the ECG simulator and the MUSIC database, and Sec. IV presents the results, notably on the prediction of SCD. Section V discusses the results and Sec. VI provides the main conclusions.

II. METHODS

A. Multilead ECG enhancement using πCA

A multilead strategy based on πCA is employed for the purpose of improving QT delineation and, ultimately, QT adaptation. The strategy involves a spatial linear transformation designed to emphasize T-wave periodicity, and, consequently, to attenuate f-waves, by exploiting spatial and temporal information in the ECG. In mathematical terms, the transformation is given by

$$y(n) = \mathbf{w}^T \mathbf{x}(n), \tag{1}$$

where the vector $\mathbf{x}(n) = \begin{bmatrix} x_1(n) & \cdots & x_L(n) \end{bmatrix}^T$ contains the ECG samples observed at time n in L leads subjected to band-pass filtering to remove baseline wander and attenuate muscle noise (cutoff frequencies at 0.5 and 35 Hz). The weights $\mathbf{w} = \begin{bmatrix} w_1 & \cdots & w_L \end{bmatrix}^T$ are determined by a generalized variant of πCA, and the transformed lead $y(n)$ is used for delineation.

While the transformation in (1) is applied to every sample of the ECG signal, $\mathbf{w}$ is determined from a data matrix containing only the samples of the T-wave interval, starting D samples after the k-th QRS fiducial point $n_{\text{QRS},k}$ and lasting for M samples in a selecting learning period (D and M are set to 80 and 350 ms, respectively). By restricting the data matrix to containing T-waves only, the periodic property of the T-wave is emphasized. The inclusion of other waves in the learning phase, i.e., the P-wave and/or the QRS complex, could go against the periodicity criterion, since the periodicity of the P-wave and the QRS complex can present spatial directions other than those related to the T-wave periodicity. If this is the case, πCA will result in an intermediate spatial direction, not necessarily the one which is the optimal for the T-wave spatial structure.

For the k-th T-wave interval, the M samples of the L leads are contained in the $L \times M$ data matrix

$$\mathbf{X}_k = \begin{bmatrix} \mathbf{x}_k(0) & \cdots & \mathbf{x}_k(M-1) \end{bmatrix}, \tag{2}$$

where

$$\mathbf{x}_k(m) = \begin{bmatrix} x_1(n_{\text{QRS},k} + D + m) \\ \vdots \\ x_L(n_{\text{QRS},k} + D + m) \end{bmatrix}, \quad m = 0, \ldots, M-1. \tag{3}$$

Starting at the q-th T-wave, an ensemble of B consecutive T-waves is contained in the $L \times MB$ ensemble data matrix

$$\mathbb{X}_q = \begin{bmatrix} \mathbf{X}_q & \cdots & \mathbf{X}_{q+B-1} \end{bmatrix}. \tag{4}$$

Thus, the l-th row of $\mathbb{X}_q$ contains B concatenated T-waves of the l-th lead.

The proposed approach to T-wave enhancement builds on the fact that the T-wave is 1-to-P-beat periodic, meaning that it is 1-2-$\cdots$-P beat periodic. In the following, this approach is referred to as generalized πCA (GπCA$_P$), where 1-to-P-beat periodic components are projected onto the transformed lead $y(n)$, while components with other periodicities, e.g., f-waves, or without any obvious periodicity, e.g., muscle noise, are not. To maximize the 1-to-P-beat periodicity, the generalized Rayleigh quotient is minimized with respect to $\mathbf{w}$:

$$\epsilon_P(\mathbf{w}) = \frac{\sum_{p=1}^{P} \|\mathbf{w}^T \mathbb{X}_{q+p} - \mathbf{w}^T \mathbb{X}_q\|^2}{\|\mathbf{w}^T \mathbb{X}_q\|^2}$$
$$= \frac{\mathbf{w}^T \mathbf{R}_{\Delta \mathbb{X}_q}^P \mathbf{w}}{\mathbf{w}^T \mathbf{R}_{\mathbb{X}_q} \mathbf{w}}, \tag{5}$$

where $\mathbf{R}_{\Delta \mathbb{X}_q}^P$ is a generalized spatial correlation matrix characterizing the 1-to-P-beat periodicity, defined by

$$\mathbf{R}_{\Delta \mathbb{X}_q}^P = \frac{1}{PBM} \sum_{p=1}^{P} \Delta \mathbb{X}_{p,q} \, \Delta \mathbb{X}_{p,q}^T, \quad P \geq 1, \tag{6}$$

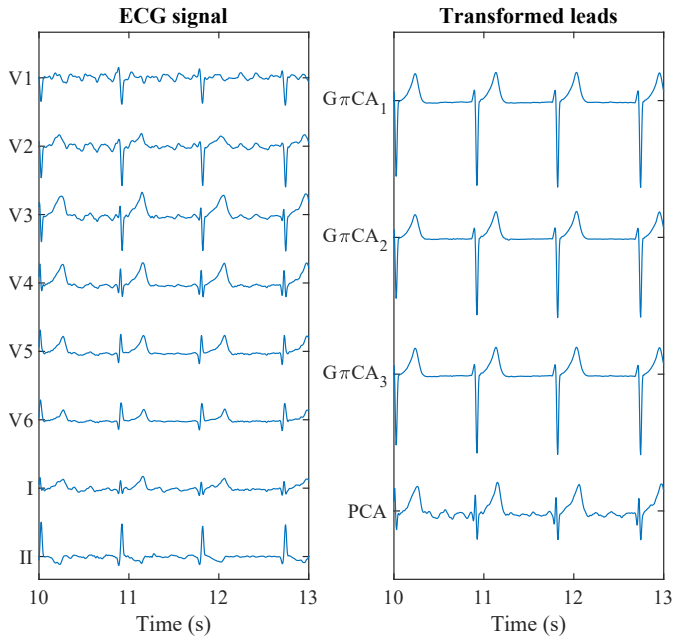$$\Delta \mathbb{X}_{p,q} = \mathbb{X}_{q+p} - \mathbb{X}_q, \tag{7}$$

Fig. 1: Example of standard ECG leads (V1–V6, I, II), and transformed leads obtained using GπCA$_P$, $P = 1, 2, 3$, and PCA ($B = 64$).

and $\mathbf{R}_{\mathbb{X}_q}$ is the spatial correlation of $\mathbb{X}_q$, defined by

$$\mathbf{R}_{\mathbb{X}_q} = \frac{1}{BM}\mathbb{X}_q\mathbb{X}_q^T. \qquad (8)$$

The generalized Rayleigh quotient is minimized by the eigenvector with the smallest eigenvalue that results from solving the generalized eigenvalue problem, given by

$$\mathbf{R}_{\Delta\mathbb{X}_q}^P \mathbf{w}^* = \lambda \mathbf{R}_{\mathbb{X}_q} \mathbf{w}^*. \qquad (9)$$

Consequently, the optimal weights in (1) are given by that particular eigenvector, denoted $\mathbf{w}^*$. When processing an entire recording, a selected set, starting at beat q, of B consecutive T-waves from beats with dominant morphology are used for learning $\mathbf{w}^*$. Then, the remaining part of the recording is analyzed using $\mathbf{w}^*$.

For comparison, the spatial version of principal component analysis (PCA) is implemented, where the optimal weights are given by the eigenvector of $\mathbf{R}_{\mathbb{X}_q}$ corresponding to the largest eigenvalue [26].

Figure 1 illustrates the lead transformation when either GπCA$_P$ or PCA is applied to the standard ECG leads. While residual f-waves are present in the PCA-transformed lead, they are completely removed in the GπCA-transformed leads. The differences among the GπCA-transformed leads are negligible.

B. QT delineation

A single-lead, wavelet-based algorithm [27] is employed for QRS detection as well as for QT delineation of original and transformed leads. For the k-th QRS complex, the following points in time are determined: QRS fiducial point $n_{\text{QRS},k}$, QRS onset $n_{\text{QRSo},k}$, and T-wave end $n_{\text{Te},k}$. It should be noted that the fiducial point $n_{\text{QRS},k}$ is subject to refinement using crosscorrelation-based time alignment.
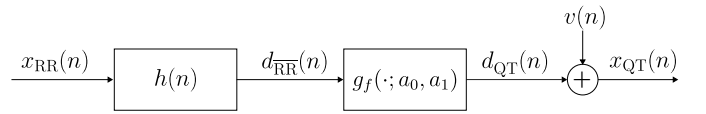

Fig. 2: Block diagram describing the relation between QT and RR intervals. The model is composed of an FIR filter with impulse response $h(n)$, followed by a memoryless function $g_f(\cdot; a_0, a_1)$. Adapted from [9].

Both the RR interval series $(n_{\text{QRS},k} - n_{\text{QRS},k-1})$ and the QT interval series $(n_{\text{Te},k} - n_{\text{QRSo},k})$ are evenly resampled at a rate of 4 Hz, resulting in $x_{\text{RR}}(n)$ and $x_{\text{QT}}(n)$, respectively. Before resampling, outliers in the QT interval series are excluded using the median absolute deviation. The two series are then lowpass filtered with a cutoff frequency of 0.25 Hz.

C. QT adaptation to heart rate changes

The relation between RR intervals $x_{\text{RR}}(n)$ and observed QT intervals $x_{\text{QT}}(n)$ is modeled by the system displayed in Fig. 2, composed of an FIR filter followed by a memoryless function and additive noise [9]. The FIR filter, of length N with impulse response $h(n)$, $n = 0, \ldots, N-1$, describes how the current QT interval depends on the preceding RR intervals ("QT memory"); N is set to 1200, i.e., 300 s. The function $g_f(\cdot; a_0, a_1)$ accounts for the memoryless, possibly nonlinear relation between the filter output $d_{\overline{\text{RR}}}(n)$ and the QT intervals $d_{\text{QT}}(n)$. This function is given by one of the functions f contained in the set $\Omega_f \equiv \{$linear, hyperbolic, parabolic, logarithmic, shifted logarithmic, exponential, arcus tangent, hyperbolic tangent, arcus hyperbolic sine, and arcus hyperbolic cosine$\}$, all parametrized by a_0 and a_1 [9]. After adding the noise term $v(n)$, accounting for delineation and modeling errors, the observed QT intervals are modeled by

$$\begin{aligned} x_{\text{QT}}(n) &= d_{\text{QT}}(n) + v(n) \\ &= g_f\left(d_{\overline{\text{RR}}}(n); a_0, a_1\right) + v(n), \end{aligned} \qquad (10)$$

where

$$d_{\overline{\text{RR}}}(n) = x_{\text{RR}}(n) * h(n). \qquad (11)$$

For each patient, the model parameters are determined by minimizing the regularized least squares criterion, using a global optimization algorithm based on the direct method [28]. Since this is an inverse "ill-posed" problem, the regularization includes a priori information of the solution to produce more accurate estimates [29]. The regularized least squares estimator is given by [9], [30]:

$$\{\hat{\mathbf{h}}, \hat{f}, \hat{a}_0, \hat{a}_1\} = \arg \min_{\{\mathbf{h},f,a_0,a_1\}} J(\mathbf{h}, f, a_0, a_1), \qquad (12)$$

where

$$J(\mathbf{h}, f, a_0, a_1) = \|\mathbf{d}_{\text{QT}} - \mathbf{x}_{\text{QT}}\|^2 + \beta^2\|\mathbf{D}\mathbf{h}\|^2, \qquad (13)$$

$$\mathbf{d}_{\text{QT}} = \begin{bmatrix} d_{\text{QT}}(N) \\ \vdots \\ d_{\text{QT}}(N_T - 1) \end{bmatrix}, \qquad (14)$$

$$\mathbf{x}_{\mathrm{QT}} = \begin{bmatrix} x_{\mathrm{QT}}(N) \\ \vdots \\ x_{\mathrm{QT}}(N_T - 1) \end{bmatrix}, \qquad (15)$$

N_T the total number of samples in the QT-RR series, and $\mathbf{h} = \begin{bmatrix} h(0) & \cdots & h(N-1) \end{bmatrix}^T$.

Before estimation can take place, the Tikhonov matrix $\mathbf{D}$ and β^2, defining the regularization, need to be determined. The matrix $\mathbf{D}$ is designed to enforce an exponential decay of $h(n)$:

$$\tilde{h}(n) = \frac{(1 - \alpha)}{(1 - \alpha^N)} \alpha^n, \quad n = 0, \ldots, N - 1, \qquad (16)$$

where $\tilde{h}(n)$ has unit gain at zero frequency and $0 < \alpha < 1$. Deviations from the exponential decay are penalized by the following matrix structure:

$$\mathbf{D} = \begin{bmatrix} \alpha & -1 & 0 & 0 & \ldots & 0 & 0 \\ 0 & \alpha & -1 & 0 & \ldots & 0 & 0 \\ \vdots & & & \ddots & & & 0 \\ 0 & 0 & 0 & 0 & \ldots & \alpha & -1 \end{bmatrix}. \qquad (17)$$

Note that for $h(n) = \tilde{h}(n)$, $\|\mathbf{Dh}\| = 0$. The parameter α is estimated as the exponential decay that best fits $h(n)$ using $f = $ 'linear'. Once α has been estimated, β^2 is determined from (13) with $f = $ 'linear' and using the "L-curve" criterion [31]. It controls the weight assigned to the regularization energy $\|\mathbf{Dh}\|^2$ relative to the residual energy $\|\mathbf{d}_{\mathrm{QT}} - \mathbf{x}_{\mathrm{QT}}\|^2$, being the energy of $v(n)$.

D. Risk markers

Two parameters are considered for risk stratification, both describing QT adaptation. Based on $h(n)$, the parameter L_{90} is defined to cover 90% of the total memory. Thus, the highest sample index for which the cumulative sum

$$H(j) = \sum_{k=j}^{N-1} h(k), \quad j = 0, \ldots, N - 1, \qquad (18)$$

exceeds $\eta = 0.1$ is identified and denoted L_{90} (expressed in seconds) [9].

Since $\tilde{h}(n)$ is a first-order system, it is fully characterized by the time lag

$$\tau = -\frac{1}{\ln(\alpha)}. \qquad (19)$$

The advantage of using τ over L_{90} is computational efficiency, as neither β^2 nor f have to be determined.

E. Statistical analysis of results from real ECGs

Data are presented as mean±standard deviation for continuous variables, unless otherwise specified. Two-tailed Mann–Whitney and Fisher exact tests were used for univariate comparison of quantitative and categorical data, respectively, between SCD and non-SCD groups. Survival analysis was performed using the Kaplan–Meier estimator and comparison of cumulative events by the log-rank test. The prognostic value of τ and L_{90} in predicting SCD was determined with univariate and multivariate Cox proportional hazards analysis. For all tests, the null hypothesis was rejected for $p \leq 0.05$.

III. Materials

A. Simulated data

QT delineation performance was evaluated standard leads (V1–V6, I, II) and orthogonal leads (X, Y, Z) generated by the AF simulator in [32]. The simulator accounts for important characteristics such as switching between sinus rhythm and AF, varying P-wave morphology, repetition rate of f-waves, and various types of noise. In the present study, however, the simulated signals were always in AF (permanent AF), and thus no switching takes place.

Since the simulator does not account for QT adaptation, it was updated so that QT intervals are nonlinearly resampled according to the hyperbolic model. In addition, the updated simulator accounts for morphological variability of QRST complexes due to respiration as proposed in [33].

The QRS-to-f-wave signal-to-noise ratio (SNR) is defined in lead l as

$$\mathrm{SNR}_l = 20 \cdot \log_{10}\left(\frac{A_{\mathrm{QRS},l}}{A_{f,l}}\right), \qquad (20)$$

where $A_{\mathrm{QRS},l}$ is the peak-to-peak amplitude of the ensemble averaged QRS of lead l (determined in a 100-ms interval centered around $n_{\mathrm{QRS},k}$) and $A_{f,l}$ is the peak-to-peak f-wave amplitude of lead l, computed as the mean of the difference between the upper and the lower envelope of the f-waves [33]. Real noise with $20\,\mu\mathrm{V}$ RMS was added to make the simulated ECG more realistic [32].

To evaluate the influence of f-wave amplitude on QT delineation and estimation of τ, 15 1-h ECGs were generated. The performance was evaluated at different SNRs (15, 18, 21, and 24 dB) by rescaling the f-wave amplitude. The global SNR was determined by the lead with lowest SNR. The exponential profile was defined by setting $\alpha = e^{\frac{1}{\tau}}$ and $\tau = 25$ s [34].

The reference beat-to-beat QT series $x_{\mathrm{QT}}^r(k)$ was obtained from delineation before f-waves and noise are added. Thus, the QT delineation error in lead l was computed before interpolation of the series as

$$e_{\mathrm{QT},l}(k) = x_{\mathrm{QT},l}(k) - x_{\mathrm{QT},l}^r(k). \qquad (21)$$

Each reference series was also used for computation of the reference τ^r. The error in the time lag τ in lead l was

$$e_{\tau,l} = \hat{\tau}_l - \hat{\tau}_l^r. \qquad (22)$$

The number of T-waves was set to $B = 64$ and $q = 1$.

B. Real ECG data

The proposed method was also evaluated on ambulatory ECG recordings (24-h Holter) acquired from patients with chronic heart failure (CHF) with permanent AF, recruited for the prospective multicenter MUSIC (MUerte Súbita en Insuficiencia Cardiaca) study [25]. Out of the original cohort of 992 consecutive patients with symptomatic CHF, belonging to functional classes II and III of the New York Heart Association (NYHA) classification, 171 patients (43 females, 68.9±10.4 years old) were selected for the present study.

Data for demographic and clinical characteristics and medication were collected at the time of enrolment. In the AF subgroup, 71.3% were classified as NYHA class II with average left ventricular ejection fraction (LVEF) of 39.4±15.7%, and 50.9% of them had reduced LVEF ($\leq 35\%$). Ischemic etiology of CHF was present in 26.9% of patients and intraventricular conduction delay (QRS duration >0.12 s) in 41.5% of patients. The main patient characteristics of the study group are summarized in Table I. The orthogonal leads were acquired at a sampling rate of 200 Hz using SpiderView recorders (ELA Medical, Sorin Group, France).

A follow-up period was conducted for an average of 48 months, including periodic visits every 6 months. At the end of the follow-up period, the study group included 19 SCDs, 24 deaths due to a different cardiac origin, 20 non-cardiac deaths and 108 survivors. SCD was defined by the study's end point committee. The study protocol was approved by the institutional ethical boards and all patients signed an informed consent [25].

The time lag parameters τ and L_{90} were estimated in 1-h windows, after which the median was computed to characterize each patient. The number of T-waves was set to $B = 128$. In order to obtain reliable parameter estimates, at least 90% of the B beats needed to: i) be labelled as normal beats by the Aristotle software [35]; and ii) have a difference in baseline voltage between two successive beats less than 300 μV [36]. The index q was determined by the first segment within the recording fulfilling these two criteria.

TABLE I: Clinical characteristics of the study population. Data are expressed as mean±standard deviation for continuous variables and as absolute number (percentage) for categorical variables.

|	Overall population (n = 171)	SCD (n = 19)	Non-SCD (n = 152)
Age (years)	68.9±10.4	69.2±10.5	68.9±10.4
Gender (males)	128 (74.8%)	16 (84.2%)	112 (73.7%)
LVEF $\leq 35\%$	87 (50.9%)	14 (73.7%)	73* (48.0%)
NYHA class III	49 (28.6%)	5 (26.3%)	44 (28.9%)
Diabetes	50 (29.2%)	6 (31.6%)	44 (28.9%)
Beta blockers	100 (58.5%)	9 (47.3%)	91 (59.9%)
Amiodarone	25 (14.6%)	2 (10.5%)	23 (15.1%)
Digoxin	106 (62.0%)	11 (57.9%)	95 (62.5%)
QRSd ≥ 120 ms	71 (41.5%)	11 (57.9%)	60 (39.5%)
QTc ≥ 450 ms	76 (44.4%)	5 (26.3%)	71 (46.7%)

*$p \leq 0.05$ SCD vs. non-SCD
LVEF: Left ventricular ejection fraction; NYHA: New York Heart Association
QRSd: QRS duration; QTc: corrected QT interval.

IV. RESULTS

A. QT delineation and adaptation performance

With the goal to determine P, the errors e_{QT} and e_τ were evaluated for different values of P when computing the GπCA-transformed lead. The results in Fig. 3.(a) show that e_{QT} does not differ much for $P =$ 1, 2, and 3, decreasing from $e_{QT,G\pi CA_1} = 1.8 \pm 2.7$ ms to $e_{QT,G\pi CA_3} = 1.4 \pm 2.3$ ms for SNR=24 dB. Similar results are obtained for e_τ, see Fig. 3.(b), where the variance is reduced from 0.58 s in GπCA$_1$ to 0.41 s
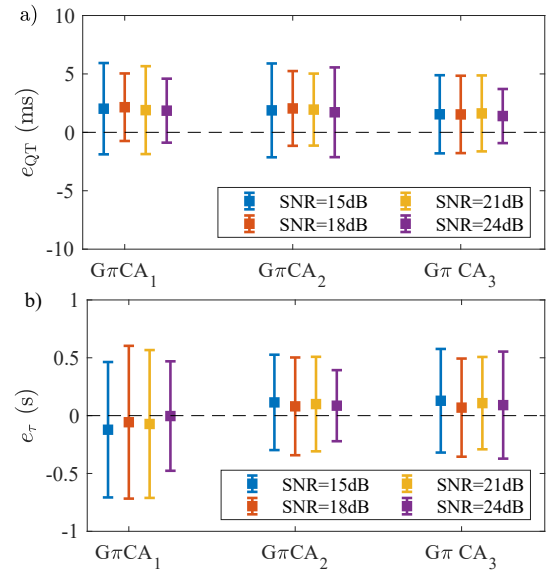
Fig. 3: (a) QT delineation error e_{QT} and (b) time lag estimation error e_τ for the GπCA-transformed lead ($P = 1, 2, 3$) using the standard leads.

in GπCA$_2$, and 0.45 s in GπCA$_3$, for SNR=12 dB. Therefore, in the following, $P = 1$ is always used as this choice is less computationally demanding.

Figure 4 shows $e_{QT,l}$ for the original and transformed leads at different SNRs. The performance is evaluated for standard leads, orthogonal leads, and related transformed leads. In general, the delineation of the original leads is worse than that of the GπCA-transformed lead. The standard leads and PCA-transformed lead exhibits a marked decreasing trend in the variance as the SNR increases, while the GπCA$_1$-transformed lead is much more robust at low SNRs. Only $e_{QT,V6}$ is comparable to GπCA$_1$, though a slightly higher variance is obtained at a low SNR. The PCA-transformed lead computed from the standard leads performs worse than does GπCA$_1$; however, this advantage becomes less obvious when using the orthogonal leads.

Figure 5 shows $e_{\tau,l}$ of the original and transformed leads at different SNRs. Similar to the results in Fig. 4, the GπCA$_1$-transformed lead outperforms the standard leads as well as the PCA-transformed lead for all SNRs except for the case of V5 and V6, for which the error variance is smaller at high SNRs (21 and 24 dB). Leads V1, V2, V3, I, and II present larger f-waves, and, therefore, the associated $e_{\tau,l}$ are also larger; only $e_{\tau,V6}$ is comparable to that of the GπCA$_1$-transformed lead ($e_{\tau,V6} = -0.1 \pm 0.7$ s). Using the orthogonal leads, the estimation error of the PCA-transformed lead is lower than that of the GπCA$_1$-transformed lead. For the lowest SNR, the corresponding errors are $e_{\tau,G\pi CA_1} = -0.03 \pm 0.84$ s and $e_{\tau,PCA} = -0.14 \pm 0.47$ s.

QT delineation is illustrated in Fig. 6. Comparing n_{QRSo} and n_{Te} with their respective reference times, a considerable disagreement is noted in V1 and V2 due to large f-waves, as well as for PCA-transformed lead, while the disagreement is smaller in the GπCA$_1$-transformed lead.
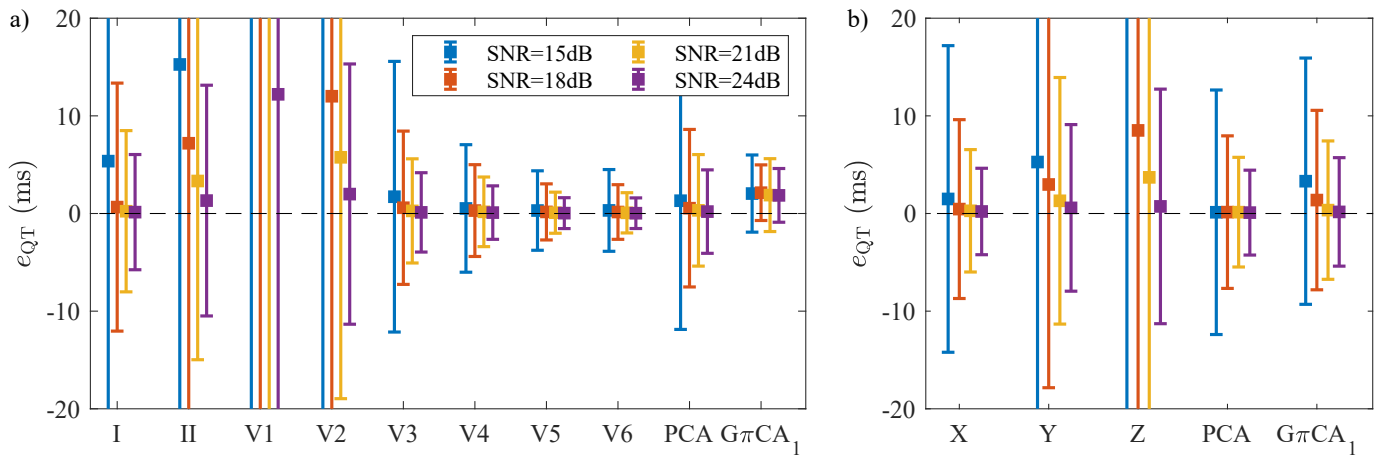
Fig. 4: Delineation error e_{QT} (mean $\pm$ standard deviation) in (a) standard leads and (b) orthogonal leads, together with transformed leads obtained by $G\pi CA_1$ and PCA.
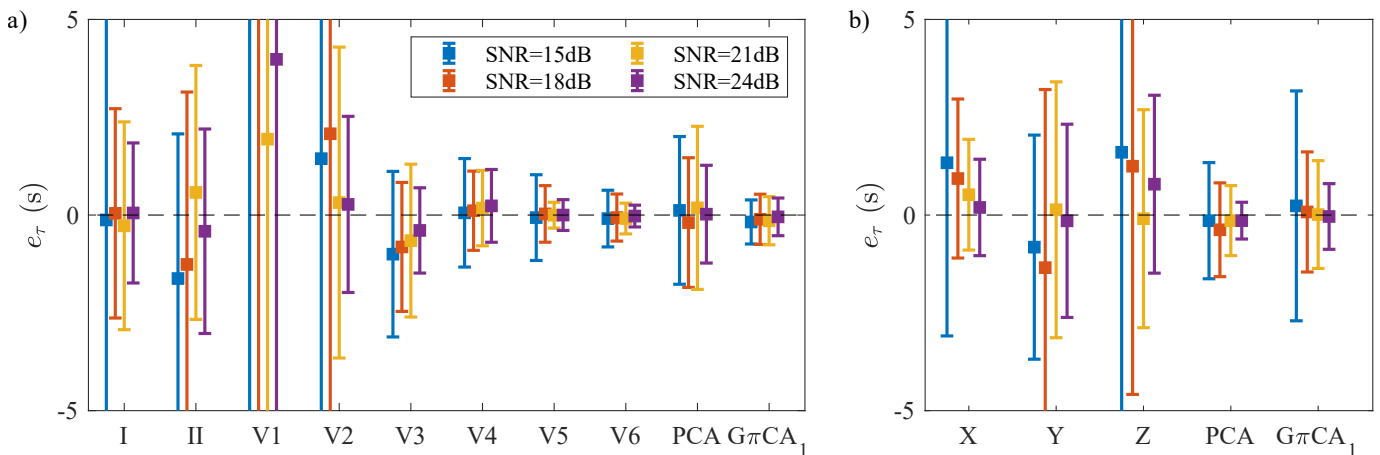

Fig. 5: Estimation error e_τ (mean $\pm$ standard deviation) in (a) standard leads and (b) orthogonal leads, together with transformed leads obtained by $G\pi CA_1$ and PCA.

B. Prognostic value of QT adaptation

Among the 10 functions in Ω_f, the linear

$$g_l(d_{\overline{RR}}(n); a_0, a_1) = a_0 + a_1 d_{\overline{RR}}(n) \qquad (23)$$

and the hyperbolic

$$g_h(d_{\overline{RR}}(n); a_0, a_1) = a_0 + \frac{a_1}{d_{\overline{RR}}(n)} \qquad (24)$$

are the ones that best fitted the data, divided into 32.4% and 64.7% of the whole population, respectively. Looking at the distribution within the non-SCD group, the corresponding percentages remain essentially the same (29.8% and 67.6%), while, in the SCD group, the corresponding percentages are 52.6% and 47.4%.

The distributions of τ and L_{90} for the non-SCD and SCD groups are presented in Fig. 7. SCD is associated with larger τ and L_{90}. However, the prolongation is only significant for $G\pi CA_1$ ($\tau_{G\pi CA_1} = 50\pm24.5$ s vs. $\tau_{G\pi CA_1} = 67.1\pm35.9$ s for non-SCD and SCD, respectively, $p = 0.021$, and $L_{90,G\pi CA_1} = 111.2\pm43.7$ s vs. $L_{90,G\pi CA_1} = 136.7\pm46.7$ s for non-SCD and SCD, respectively, $p = 0.028$).

The predictive value of τ is assessed using a risk threshold set to the 75th percentile of the total distribution of τ_l for the whole population, i.e., the group at risk, denoted as $\tau_l(+)$, is composed of the 25% of patients with the largest τ_l. This dichotomization is also done for L_{90}.

Univariate Cox proportional analysis demonstrates that the time lag $\tau_{G\pi CA_1}$ leads to the highest hazard ratio (3.49-fold increased risk in the $\tau_{G\pi CA_1}(+)$ group), followed by τ_{PCA}, see Table II. The parameter L_{90} offers the same stratification performance as $\tau_{G\pi CA_1}$ and similar for τ_{PCA}. None of the orthogonal leads are associated with SCD. LVEF is the only clinical variable associated with SCD, with a hazard ratio of 3.11. The criterion QTc$\geq$450 ms, being the most well-established ECG-based marker in clinical routine, is not predictive of SCD.

The Kaplan–Meier curves for $\tau_{G\pi CA_1}$ are shown on Fig. 8. The survival probability rate is significantly lower for patients at high risk ($\tau_{G\pi CA_1}(+)$) than for patients at low risk ($\tau_{G\pi CA_1}(-)$) at the end of the follow-up period.

A multivariate Cox model is constructed by adjusting for significant clinical covariates: age, gender, NYHA class III, LVEF$\leq$35%, and the use of antiarrhythmic drugs (beta block-
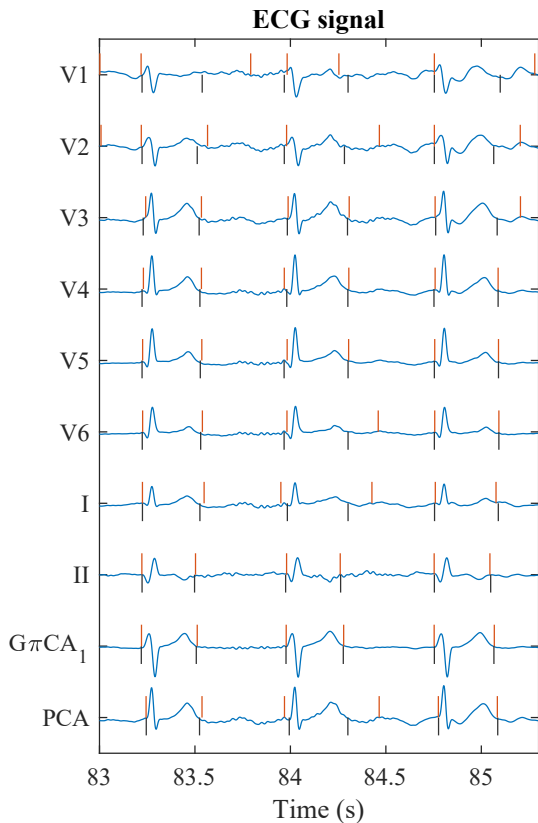
ECG signal

Fig. 6: Simulated standard ECG leads and transformed leads obtained by $G\pi CA_1$ and PCA. QRS onset and T end are indicated (red lines) together with the reference annotations (black lines).

TABLE II: Univariate and multivariate Cox models for sudden cardiac death in AF patients for τ determined in individual leads, together with corrected QT interval (QTc) and left ventricular ejection fraction (LVEF).

|	Risk threshold	Univariate HaR (95% CI)	*p*-value	Multivariate* HaR (95% CI)	*p*-value
τ_X	61.9 s	1.7 (0.65,4.48)	0.283	2.36 (0.85,6.54)	0.099
τ_Y	60.1 s	1.27 (0.46,3.52)	0.651	1.27 (0.44,3.68)	0.658
τ_Z	61.9 s	1.57 (0.59,4.13)	0.364	1.71 (0.63,4.64)	0.295
τ_{PCA}	60.1 s	**2.65** (1.06,6.60)	**0.037**	**2.74** (1.07,7.01)	**0.036**
$\tau_{G\pi CA_1}$	60.9 s	**3.49** (1.72,8.62)	**0.007**	**3.46** (1.37,8.74)	**0.009**
$L_{90,PCA}$	137 s	**3.28** (1.32,8.08)	**0.010**	**3.45** (1.33,8.94)	**0.011**
$L_{90,G\pi CA_1}$	138.6 s	**3.49** (1.72,8.62)	**0.007**	**3.51** (1.31,9.35)	**0.012**
QTc	450 ms	0.44 (0.16,1.23)	0.116	0.41 (0.14,1.16)	0.094
LVEF	≤35%	**3.11** (1.12,8.64)	**0.030**	**3.18** (1.09,9.23)	**0.034**

HaR: Hazard ratio
*Multivariate includes age, gender, New York Heart Association class III, LVEF ≤35%, beta blockers, amiodarone, and digoxin.

ers, amiodarone, and digoxin). After adjustment, $\tau_{G\pi CA_1}$ and $L_{90,G\pi CA_1}$ are the most significant variables with the highest hazard ratio associated with SCD, see Table II.

Fig. 9 illustrates how the QT intervals adapt to RR interval changes for a patient in the MUSIC database.

V. DISCUSSION

The present study addresses the problem of QT interval delineation in the presence of f-waves by proposing a novel multilead strategy based on periodic component analysis to enhance T-waves over f-waves. The results from a simulation study show that the proposed method provides more accurate QT delineation and time lag estimation than does the single-lead approach. The prognostic value of the QT adaptation time lag has been assessed in a CHF population and permanent AF, where a prolonged adaptation time of the QT interval to heart rate changes has been associated with a high risk for SCD.

Since the focus is the estimation of τ, the SNR was defined by the QRS- and f-wave amplitudes, cf. (20), rather than by the f-wave amplitude and the noise level. Since the noise level was held fixed at 20 μV for all simulations, a future study may investigate how performance is influenced by higher noise levels. It should be noted though that the spatial definition of πCA has been found robust in the presence of noise and body position changes [24].

The potential of $G\pi CA$ in separating beat-periodic components from f-waves and noise depends on the number of leads available for analysis. The results from the simulation study were obtained using either the standard leads or the orthogonal leads. The results show that the orthogonal leads are associated with larger QT delineation and time lag errors compared to those of the standard leads. Only leads V5 and V6, which are the most distal to the atria, provide better performance (lower variance) than $G\pi CA_1$ at high SNRs. Still, at low SNRs (15 dB) the benefit in terms of variance is more evident. Nonetheless, the benefit of using lead V5 or V6 may still be compromised by the signal quality along the whole recording, i.e., the presence of motion artifacts and muscle noise, or electrode unattachment. Another factor of practical importance is that very few Holter devices record the standard 12-lead ECG. Provided that more than one lead is available, multilead πCA will overcome this limitation by combining the set of available leads, maximizing the periodic components over any other sources of noise, without needing any a priori lead selection.

Both bias and variance of $e_{QT,G\pi CA_1}$ remain essentially the same for all SNRs, see Fig. 4. For the transformed leads, the reference QT series is obtained from delineation of the transformed clean ECG signal, before adding f-waves and noise. On the other hand, the QT series obtained from delineation of the transformed noisy signal is obtained from transforming the noisy leads, not the clean leads. Consequently, $\mathbf{w}^*$ differs slightly between these two cases, implying that a certain bias is introduced since the T-wave morphology may differ slightly. In any case, the mean error is less than 2 ms, which is about the same as the error between expert cardiologists [37]. It should be noted that the estimation of τ is invariant to bias in the QT
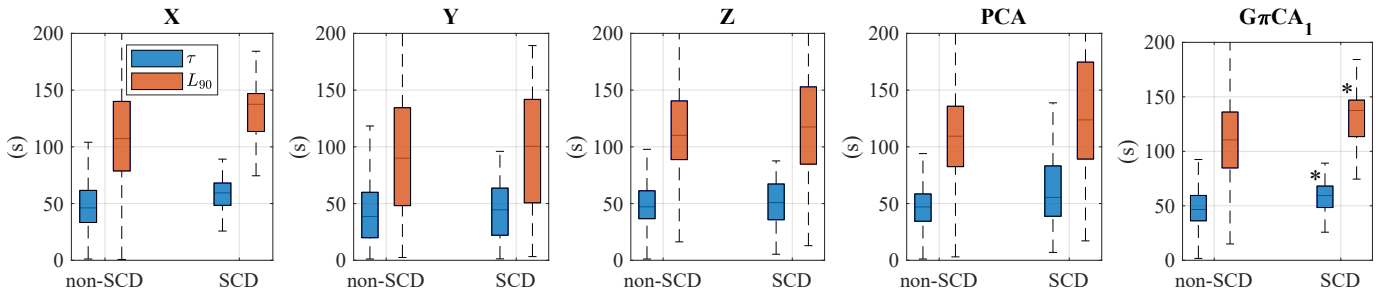
Fig. 7: Distribution of τ (blue) and L_{90} (red) for non-SCD and SCD groups in orthogonal leads and transformed leads. *: $p < 0.05$, SCD vs. non-SCD, Mann–Whitney test.
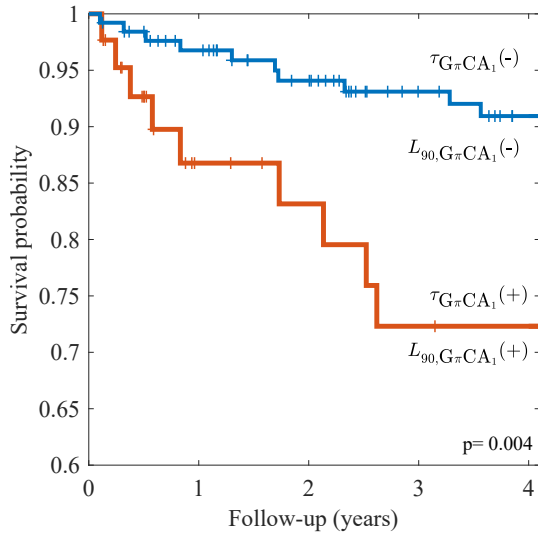
Fig. 8: Kaplan–Meier survival estimates for SCD associated with $\tau_{G\pi CA_1}$ and $L_{90,G\pi CA_1}$, which completely coincide. The survival probability curve for the $\tau_{G\pi CA_1}(-)/L_{90,G\pi CA_1}(-)$ group (blue) and the $\tau_{G\pi CA_1}(+)/L_{90,G\pi CA_1}(+)$ group (red) are represented.
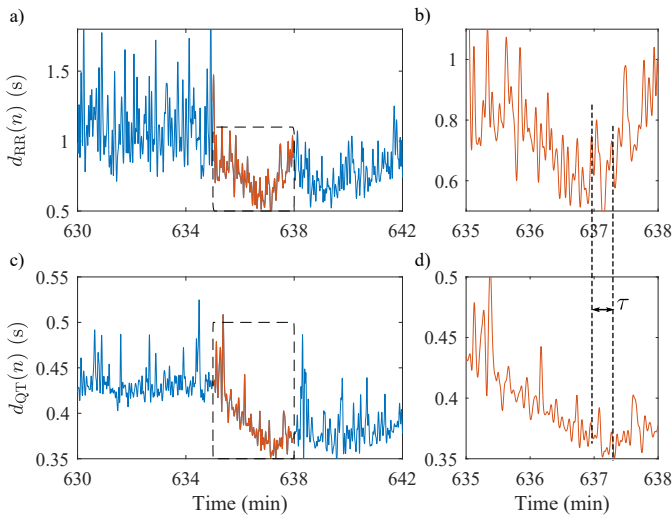
Fig. 9: (a) RR interval and (c) QT interval series extracted from a Holter recoding of the MUSIC database, together with a close-up of the red zones, (b) and (d), where the time lag between the two series is indicated.

interval delineation.

The generalized variant of πCA was introduced with the aim to improve the quality of the spatial correlation matrix $\mathbf{R}^P_{\Delta \mathbb{X}_q}$ in (6) by using more data. However, the simulation results suggest that QT delineation does not significantly improve for $P > 1$, probably due to the large number of beats used for estimating $\mathbf{R}^P_{\Delta \mathbb{X}_q}$. Had much fewer beats been used, it is likely that the quality of $\mathbf{R}^P_{\Delta \mathbb{X}_q}$ would have improved as more terms are added to the sum in (6).

Due to the irregular rhythm in AF, the location of the T-wave interval will vary from beat to beat as will its onset relative to the QRS fiducial point. Such variation is undesirable when estimating $\mathbf{w}^*$, and, therefore, the results were also computed following alignment of the T-wave intervals before forming $\mathbb{X}_q$, using the location of the T-wave peak as fiducial point. However, the alignment did not contribute to reducing the delineation errors and therefore the results are not presented.

Despite evidence that AF is associated with risk for SCD, being proarrhythmic in the ventricles [38], most of the ECG-based risk indices of ventricular repolarization heterogeneity have required sinus rhythm for proper assessment. Therefore, this study is crucial as it demonstrates the prognostic value of QT adaptation in CHF-AF patients as quantified by L_{90} and τ. In contrast to the analysis of the leads X, Y, and Z individually, only τ estimated from using all three leads transformed with either PCA or GπCA$_1$ was associated with SCD, see Fig. 8. The best stratification performance is achieved by using GπCA$_1$, where the risk group has 3.49 times increased risk than the low-risk group (hazard ratio 1.32 times higher than the one obtained by PCA). Since the ECG has a quasi-periodic structure, the enhancement of the T-wave before QT delineation, particularly the T-wave end, using a periodicity criteria is shown to outperform PCA, also in terms of predictive value.

The predictive value of τ and L_{90} is shown to be identical for the study population. This is expected as both parameters quantify the time lag either using the exponential approximation $\tilde{h}(n)$ or the estimated impulse response $\hat{h}(n)$, respectively, with the advantage that $\hat{\tau}$ comes with much less computations, cf. Sec. II-D. Both parameters are highly correlated (Pearson's and Spearman's correlation coefficients $r^2 = 0.92$ and $\rho^2 = 0.99$, respectively). Although there is a clear linear relationship between both parameters, see Fig. 10, the non-linear trend observed for large values of $\hat{\tau}$ indicates better robustness of
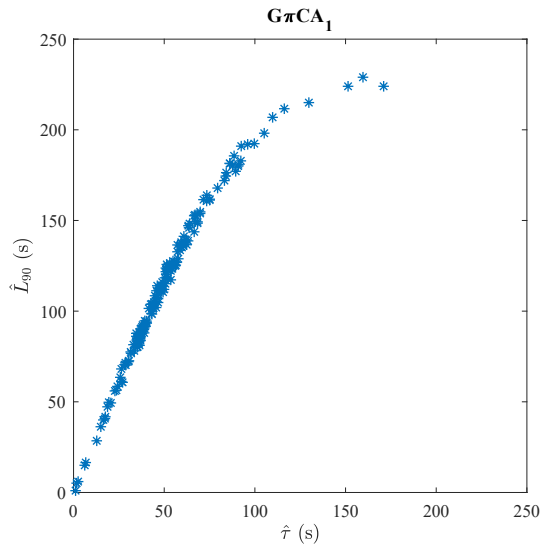
Fig. 10: Scatterplot of $\hat{L}_{90}$ versus $\hat{\tau}$ in the $G\pi CA_1$-transformed lead.

$\hat{L}_{90}$ to outliers.

Although LVEF is known to be unspecific in SCD prediction, low LVEF is associated with high risk for SCD overall. Among the most relevant clinical and pharmacological available data, only LVEF≤35% was associated with SCD outcome in our study population. However, hazard ratios in univariate and multivariate analysis were lower than the ones obtained for the proposed time lag parameters.

A limitation of the present study is the imbalance of SCD events ($n = 19$) and non-SCD events ($n = 152$) in the study population. Although the prognostic value of τ and L_{90} has been demonstrated, prospective studies are still needed in order to corroborate the clinical value of τ and L_{90}.

In contrast to sinus rhythm studies, scarce data on SCD stratification in AF is available, particularly when based on the assessment of ventricular repolarization instability. A previous study in the same cohort of patients showed that enhanced ventricular repolarization beat-to-beat variability of the ST-T complex, based on an instantaneous local alternans measurement, was associated with a higher SCD incidence [39]. The prognostic value of the indices proposed in [39] (hazard ratios between 2.66 and 3.76) is comparable to the ones reported for τ and L_{90}. However, while the approach presented in [39] requires that consecutive beats preceded by a similar RR interval are subject to bin selection, challenging in AF, the computation of τ and L_{90} is straightforward, and likely more stable.

It is well-known that other factors than HR contribute QT modulation, including the autonomic nervous system (ANS). Elucidation of the direct and indirect effects of ANS activity on the QT interval may also help assessing arrhythmia susceptibility [40]. In sinus rhythm, direct ANS influence on the ventricles is usually assessed through QT variability (QTV) analysis, adjusted by HRV. However, ventricular rate lacks ANS modulation during. Therefore, QTV analysis in AF may be a tool to directly assess any ANS effect on ventricular

repolarization. In such cases, the use of πCA need to be further studied. Indeed, it is tempting to believe that πCA is disadvantageous to use as non-periodic components are attenuated. However, beat-to-beat variations in the QT interval will be emphasized or attenuated in the πCA-transformed lead depending on how these non-periodic QTV components project onto the spatial direction of the transformed lead. This could happen even if the transformation is designed to emphasize periodicity.

VI. CONCLUSIONS

This study shows that a multilead strategy based on πCA outperforms the standard leads and PCA-transformed lead when delineating QT intervals in the presence of f-waves. Moreover, it is shown that the time lag $\tau_{G\pi CA_1}$ of the QT adaptation to HR is associated with SCD in a population of CHF patients with permanent atrial fibrillation, being the best predictor among other classical ECG-derived (QTc) and clinical variables. Therefore, it is concluded that this strategy is useful to assess QT adaptation in permanent AF, indicating that SCD risk markers developed for sinus rhythm are equally suitable for AF.

REFERENCES

[1] G. Yi *et al.*, "Circadian pattern of QT/RR adaptation in patients with and without sudden cardiac death after myocardial infarction," *Ann. Noninvasive Electrocardiol.*, vol. 4, pp. 286–294, 1999.

[2] P. Smetana *et al.*, "Individual patterns of dynamic QT/RR relationship in survivors of acute myocardial infarction and their relationship to antiarrhythmic efficacy of amiodarone," *J. Cardiovasc. Electrophysiol.*, vol. 15, pp. 1147–1154, 2004.

[3] S. Viskin *et al.*, "The response of the QT interval to the brief tachycardia provoked by standing: A bedside test for diagnosing long QT syndrome," *J. Am. Coll. Cardiol.*, pp. 1955–1961, 2010.

[4] A. Barsheshet *et al.*, "Genotype-specific QT correction for heart rate and the risk of life-threatening cardiac events in adolescents with congenital long-QT syndrome," *Heart Rhythm*, vol. 8, pp. 1207–1213, 2011.

[5] S. Seethala *et al.*, "QT adaptation and intrinsic QT variability in congenital long QT syndrome," *J. Am. Heart Assoc.*, vol. 4, 2015.

[6] H. Gravel *et al.*, "Clinical applications of QT/RR hysteresis assessment: A systematic review," *Ann. Noninvasive Electrocardiol.*, vol. 23, p. e12514, 2018.

[7] C. P. Lau *et al.*, "Hysteresis of the ventricular paced QT interval in response to abrupt changes in pacing rate," *Cardiovasc. Res.*, vol. 22, pp. 67–72, 1988.

[8] V. N. Batchvarov *et al.*, "QT–RR relationship in healthy subjects exhibits substantial intersubject variability and high intrasubject stability," *Am. J. Physiol. Heart Circ. Physiol.*, vol. 282, pp. H2356–H2363, 2002.

[9] E. Pueyo *et al.*, "Characterization of QT interval adaptation to RR interval changes and its use as a risk-stratifier of arrhythmic mortality in amiodarone-treated survivors of acute myocardial infarction," *IEEE Trans. Biomed. Eng.*, vol. 51, no. 9, pp. 1511–1520, 2004.

[10] E. Pueyo, M. Malik, and P. Laguna, "A dynamic model to characterize beat-to-beat adaptation of repolarization to heart rate changes," *Biomed. Signal Process. Control*, vol. 3, pp. 29–43, 2008.

[11] J. Halámek *et al.*, "Use of a novel transfer function to reduce repolarization interval hysteresis," *J. Interv. Card. Electrophysiol.*, vol. 29, pp. 23–32, 2010.

[12] V. Jacquemet *et al.*, "Evaluation of a subject-specific transfer-function-based nonlinear QT interval rate-correction method," *Physiol. Meas.*, vol. 32, pp. 619–635, 2011.

[13] A. Cabasson, O. Meste, and J.-M. Vesin, "Estimation and modeling of QT-interval adaptation to heart rate changes," *IEEE Trans. Biomed. Eng.*, vol. 59, pp. 956–965, 2012.

[14] A. Vinet *et al.*, "Estimation of the QT–RR relation: trade-off between goodness-of-fit and extrapolation accuracy," *Physiol. Meas.*, vol. 38, pp. 397–419, 2017.

[15] F. A. Ehlert *et al.*, "Relation between QT and RR intervals during exercise testing in atrial fibrillation," *Am. J. Cardiol.*, vol. 70, pp. 332–338, 1992.

[16] J. H. Indik *et al.*, "Bazett and Fridericia QT correction formulas interfere with measurement of drug-induced changes in QT interval," *Heart Rhythm*, vol. 3, pp. 1003–1007, 2006.

[17] C. E. Larroude *et al.*, "Beat-to-beat QT dynamics in paroxysmal atrial fibrillation," *Heart Rhythm*, vol. 3, no. 6, pp. 660–664, 2006.

[18] A. Fujiki *et al.*, "QT/RR relation during atrial fibrillation based on a single beat analysis in 24-h Holter ECG: The role of the second and further preceding RR intervals in QT modification," *J. Cardiol.*, vol. 57, pp. 269–274, 2011.

[19] Y. Yamaguchi *et al.*, "Time-dependent changes in QT dynamics after initiation and termination of paroxysmal atrial fibrillation," *Pacing Clin. Electrophysiol.*, vol. 38, pp. 1418–1424, 2015.

[20] L. Sörnmo *et al.*, "Extraction of f waves," in *Atrial Fibrillation from an Engineering Perspective*, L. Sörnmo, Ed. Springer Nature, 2018, ch. 5, pp. 137–220.

[21] L. K. Saul and J. B. Allen, "Periodic component analysis: an eigenvalue method for representing periodic structure in speech," in *Adv. Neural. Inf. Process. Sys. 13 - Proc. NIPS 2000*, vol. 14, 2000, pp. 807–813.

[22] R. Sameni, C. Jutten, and M. B. Shamsollahi, "Multichannel electrocardiogram decomposition using periodic component analysis," *IEEE Trans. Biomed. Eng.*, vol. 55, no. 8, pp. 807–813, 2008.

[23] V. Monasterio *et al.*, "A multilead scheme based on periodic component analysis for T-wave alternans analysis in the ECG," *Ann. Biomed. Eng.*, vol. 38, no. 8, pp. 2532–2541, 2010.

[24] F. Palmieri *et al.*, "ECG-based monitoring of blood potassium concentration: Periodic versus principal component as lead transformation for biomarker robustness," *Biomed. Signal. Process. Control.*, vol. 68, p. 102719, 2021.

[25] R. Vázquez *et al.*, "The MUSIC risk score: a simple method for predicting mortality in ambulatory patients with chronic heart failure," *Eur. Heart J.*, vol. 30, no. 9, pp. 1088–1096, 2009.

[26] F. Castells *et al.*, "Principal component analysis in ECG signal processing," *EURASIP J. Adv. Signal Process.*, vol. 2007, no. 1, p. 074580, 2007.

[27] J. P. Martínez *et al.*, "A wavelet-based ECG delineator: evaluation on standard databases," *IEEE Trans. Biomed. Eng.*, vol. 51, no. 4, pp. 570–581, 2004.

[28] R. M. Lewis, V. Torczon, and M. W. Trosset, "Direct search methods: then and now," *J. Comput. Appl. Math.*, vol. 124, no. 1, pp. 191–207, 2000.

[29] G. H. Golub, P. H. Hansen, and D. P. O'Leary, "Tikhonov regularization and total least squares," *SIAM J. Matrix Analysis and Applications*, vol. 21, no. 1, pp. 1955–1961, 1999.

[30] A. Mincholé *et al.*, "Modeling and quantification of repolarization feature dependency on heart rate," *Meth. Inf. Med.*, vol. 53, no. 4, pp. 324–328, 2014.

[31] P. C. Hansen, "Analysis of discrete ill-posed problems by means of the l-curve," *SIAM Review*, vol. 34, no. 4, pp. 561–580, 1992.

[32] A. Petrėnas *et al.*, "Electrocardiogram modeling during paroxysmal atrial fibrillation: application to the detection of brief episodes," *Physiol. Meas.*, vol. 38, pp. 2058–2080, 2017.

[33] S. Kontaxis *et al.*, "ECG-derived respiratory rate in atrial fibrillation," *IEEE Trans. Biomed. Eng.*, vol. 67, pp. 905–914, 2020.

[34] C. Pérez *et al.*, "Characterization of impaired ventricular repolarization by quantification of QT delayed response to heart rate changes in stress test," in *Proc. Comput. Cardiol.*, vol. 48, 2020, pp. 1–4.

[35] G. B. Moody and R. G. Mark, "Development and evaluation of a 2-lead ECG analysis program." in *Proc. Comput. Cardiol.*, vol. 9, 1982, pp. 39–44.

[36] V. Monasterio *et al.*, "Average T-wave alternans activity in ambulatory ECG records predicts sudden cardiac death in patients with chronic heart failure." *Heart Rhythm*, vol. 9, no. 3, pp. 383–389, 2012.

[37] C. Zywietz and D. Celikag, "Testing results and derivation of minimum performance criteria for computerized ECG-analysis," in *Proc. Comput. Cardiol.*, vol. 18, 1991, pp. 97–100.

[38] V. Waldmann *et al.*, "Association between atrial fibrillation and sudden cardiac death: Pathophysiological and epidemiological insights." *Circ. Res.*, vol. 127, no. 2, pp. 301–309, 2020.

[39] A. Martín-Yebra *et al.*, "Quantification of ventricular repolarization variation for sudden cardiac death risk stratification in atrial fibrillation." *IEEE J. Biomed. Health Inform.*, vol. 23, no. 3, pp. 1049–1057, 2019.

[40] R. D. Berger, "QT variability." *J. Electrocardiol*, vol. 36, pp. 83–87, 2003.